

# Excellence in Chemistry Research

## Announcing our new flagship journal

- Gold Open Access
- Publishing charges waived
- Preprints welcome
- Edited by active scientists



## Meet the Editors of *ChemistryEurope*



**Luisa De Cola**

Università degli Studi  
di Milano Statale, Italy



**Ive Hermans**

University of  
Wisconsin-Madison, USA



**Ken Tanaka**

Tokyo Institute of  
Technology, Japan

Special  
Collection

# Conversion of Ketones into Blue-Emitting Electron-Deficient Benzofurans

Krzysztof Górski,<sup>[a]</sup> Tea Ostojić,<sup>[b]</sup> Marzena Banasiewicz,<sup>[c]</sup> Erik T. Ouellette,<sup>[d, e]</sup> Luca Grisanti,<sup>\*,[b]</sup> and Daniel T. Gryko<sup>\*,[a]</sup>

**Abstract:** A novel heavy metal-free and safe synthetic methodology enabling one-step conversion of ketones into corresponding 4,5,6,7-tetrafluorobenzofurans ( $F_4BFs$ ) has been developed. The presented approach has numerous advantageous qualities, including utilization of readily available substrates, broad scope, scalability, and good reaction yields. Importantly, some of the benzofurans prepared by this method were heretofore inaccessible by any other known transformation. Importantly, furo[2,3-*b*]pyrazines and heretofore unexplored difuro[2,3-*c*:3',2'-*e*]pyridazine can be prepared using this strategy. Spectroscopic studies reveal that for simple systems, absorption and fluorescence maxima fall

within the UV spectral range, while  $\pi$ -electron system expansion red-shifts both spectra. Moreover, the good fluorescence quantum yields observed in solution, up to 96%, are also maintained in the solid state. Experimental results are supported by density functional theory (DFT) calculations. The presented methodology, combined with the spectroscopic characteristics, suggest the possibility of using  $F_4BFs$  in the optoelectronic industry (i.e., organic light emitting devices (OLED), organic field-effect transistors (OFET), organic photovoltaics (OPV)) as inexpensive and readily available emissive or semiconductor materials.

## Introduction

Benzo[*b*]furans (benzofurans) are a class of bioactive agents with important medical applications, for example as antiviral and anticancer drugs.<sup>[1,2]</sup> Concurrently,  $\pi$ -expanded benzofurans<sup>[3-8]</sup> drive the growing interest in their optical and electronic properties. Examples of their use include Thermally Activated Delayed Fluorescence (TADF) OLED emitters, photo-

chromic materials as well as semiconductors.<sup>[9-12]</sup> Although multiple synthetic methods leading to substituted benzofurans are known,<sup>[13-16]</sup> the preparation of appropriate tetrafluoro-derivatives still remains insufficiently explored.

A number of intermolecular reactions, including catalytic processes and condensations, afford the preparation of fluorinated heteroarenes (Figure 1).<sup>[17-21]</sup> Moreover, those multistep reactions often require non-readily available fluorine-containing substrates.<sup>[22-24]</sup> On the other hand, single fluorine atom substitutions are a rare class of tetrafluoroarene synthetic method and demand properly functionalized pentafluorobenzenes (Figure 1, II).<sup>[25-31]</sup>

However, the most infrequent among cyclizations are the double fluorine substitutions, not involving prior modification of the perfluorinated subunit.<sup>[32-37]</sup> From this perspective, these transformations have been identified as attractive and affordable for potential applications.

Following earlier discoveries by Brooke, in 1979 Kobayashi and co-workers described the reaction between perfluorobenzene and benzyl-phenyl ketone in the presence of NaH in dimethylformamide (DMF), leading to the formation of corresponding  $F_4BF$  in 50% yield.<sup>[38]</sup> This double nucleophilic substitution led to expected  $F_4BFs$  also for butane-2-one, propiophenone and benzyl-methyl ketone. However, the published scope was small with only moderate yields and small scales (ca. 10 mmol). In light of these literature reports, we wondered if the scope of this process could be expanded into a broad range of interesting substituents. At the same time, it is well known that NaH and DMF, as well as NaH and dimethylacetamide (DMA), occasionally form an explosive mixture, especially on larger scales.<sup>[39,40]</sup> Thus, we embarked on a journey

[a] Dr. K. Górski, Prof. D. T. Gryko  
Institute of Organic Chemistry of Polish Academy of Sciences  
Kasprzaka 44/52, 01-224 Warsaw (Poland)  
E-mail: dtgryko@icho.edu.pl

[b] T. Ostojić, Dr. L. Grisanti  
Division of Theoretical Physics  
Ruđer Bošković Institute  
Bijenička cesta 54, 10000 Zagreb (Croatia)  
E-mail: lgrisant@irb.hr

[c] Dr. M. Banasiewicz  
Institute of Physics  
Polish Academy of Sciences  
Al. Lotników 32/46 02-668 Warszawa (Poland)

[d] E. T. Ouellette  
Department of Chemistry  
University of California Berkeley  
420 Latimer Hall, Berkeley, CA (USA)

[e] E. T. Ouellette  
Chemical Sciences Division  
Lawrence Berkeley National Laboratory  
1 Cyclotron Road, Berkeley, CA (USA)

Supporting information for this article is available on the WWW under <https://doi.org/10.1002/chem.202203464>

This publication is part of a Special Collection on aromatic chemistry in collaboration with the "19<sup>th</sup> International Symposium on Novel Aromatic Compounds (ISNA-19)".

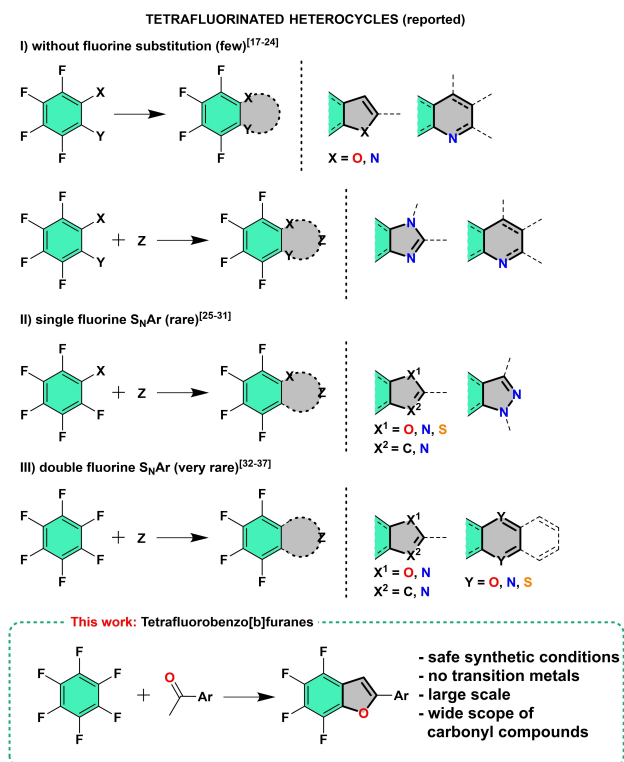


Figure 1. Synthesis of tetrafluorinated heteroaromatics.

aimed at simultaneously expanding reaction scope and modifying reaction conditions into safer ones.

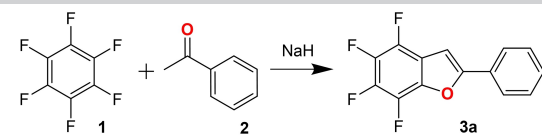
Herein, we present a straightforward, one-pot reaction for preparing F<sub>4</sub>BFs from readily available ketones. Moreover, the facile isolation of the products provides the possibility for large-scale synthesis, for example 50 mmol. These advantages open a novel path towards F<sub>4</sub>BFs, enabling exploration of both the physicochemical properties and biological properties of these systems. In view of the interesting spectrum of optical properties and the rich photophysics, we have attempted the interpretation of the observed behavior by performing DFT simulations.

## Results and Discussion

### Synthesis

The conversion of ketones into F<sub>4</sub>BFs was investigated on the model reaction between perfluorobenzene (1) and acetophenone (2) (Table 1). At the very beginning, we wanted to get acquainted with the previously known reaction conditions (NaH/DMF).<sup>[38]</sup> Upon carrying out several experiments, we observed very rapid reactions and resulting lack of reproducibility in the process. In optimization experiments, we chose to employ N-methylpyrrolidone (NMP) as a relatively inert solvent under strongly basic reaction conditions. Upon mixing the substrates with NaH and heating to 140 °C, a violent exothermic process accompanied by H<sub>2</sub> evolution and rapid reaction

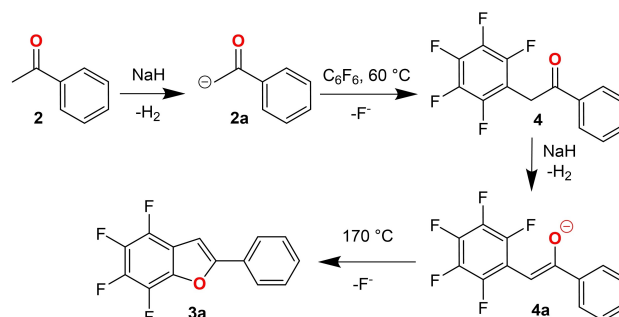
**Table 1.** Optimization of reaction conditions leading to benzofuran **3a**.



Entry <sup>[a]</sup>	Conditions	Yield [%] <sup>[b]</sup>
1	NMP (140 °C, 1 h)	6
2	NMP (0 °C, 1 h) <sup>[a]</sup>	0
3	NMP (r.t.→140 °C, 1 h) <sup>[b]</sup>	16
4	NMP (50 °C→140 °C, 1 h)	39
5	NMP (r.t.→80 °C, 1 h) <sup>[c]</sup>	30
6	THF (60 °C, 1 h)→NMP (140 °C, 1 h)	28
7	THF (60 °C, 1 h)→diglyme (170 °C, 1 h)	53
8	diglyme (60 °C, 1 h→170 °C, 1 h)	48
9	THF (60 °C, 1 h)→diglyme (170 °C, 1 h) <sup>[d]</sup>	60

Reaction conditions: 10 mmol of ketone, 15 mmol of perfluorobenzene and 25 mmol of NaH, [a] KH was used as ionizing agent, [b] all reagents were mixed prior to addition of solvent, [c] ketone was added to the mixture of reagents in NMP, [d] 50 mmol scale.

volume expansion is observed. However, under these conditions, the expected product **3a** is formed in a very low yield (Table 1, entry 1). Several factors influence the course of this reaction. First, the rapid temperature rise causes evaporation of **2**. On the other hand, a violent and unpredictable process leads to many byproducts, decreasing the reaction yield and making the effective isolation of **3a** troublesome. In turn, lowering the reaction temperature to 0 °C did not give the desired reactivity. Also, changing the ionizing agent from NaH to the more reactive KH and maintaining a 0 °C reaction temperature also initiates a violent, exothermic process leading to byproducts (Table 1, entry 2). The acquired results prompted an insightful analysis of the probable reaction mechanism, which can be provisionally divided into four main processes (Scheme 1). The first one is alkali hydride promoted ionization of ketone **2** to enolate **2a**, which turned out to be an exothermic reaction accompanied by H<sub>2</sub> evolution. The next step is a nucleophilic substitution with a fluorinated system (**4**) followed by another enolization process leading to **4a**. Finally, furan ring formation occurs (**3a**) as a result of the second fluorine atom substitution. As it turns out, manipulating both the temperature and the mixture composition give better control throughout the reaction (Table 1, entries 3–5). Indeed, enolization of **2** to **2a**, in

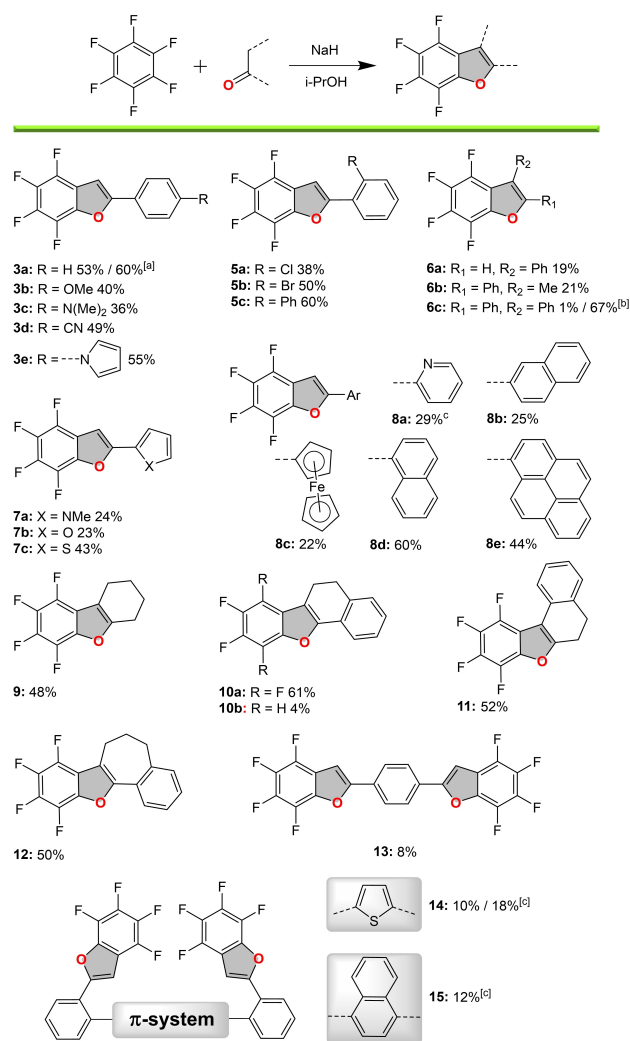


Scheme 1. Plausible reaction mechanism.

an absence of **1**, proceeds even at room temperature, though heating to 50 °C or 60 °C accelerates this relatively gentle process. After completion, an excess of **1** is introduced into the reaction mixture, leading to ketone **4**. Quenching the reaction at this stage allows easy isolation of **4** with a 61 % yield. On the other hand, due to the presence of NaH, **4** undergoes further ionization to intermediate **4a**. The final cyclization to **3a** requires higher temperatures, for example 140 °C for NMP. The described procedure improved the initial one step protocol of ketone conversion into  $F_4BF$ s from 6% up to 39%, however, a large amount of byproducts still remained in the reaction mixture. In order to minimize these, the first ionization process was conducted in tetrahydrofuran (THF) at 60 °C, while NMP was replaced by another high boiling and inert solvent, diglyme. Upon conversion of **2** to **4a** and evaporation of volatile substances, the reaction temperature can be raised to initiate proper cyclization to **3a**.

The use of NMP in this case does not lead to significant changes (Table 1, entry 6). On the other hand, replacement with diglyme increase the reaction yield up to 60% (Table 1, entries 7–9), but final cyclization requires a temperature around 170 °C. Due to the low content of byproducts, **3a** isolation is comparably easier, and the reaction itself can be carried out on larger scales (Table 1, entry 9). Importantly, the described methodology for  $F_4BF$  synthesis gives reproducible results for the first time. Moreover, overall reaction time is shortened, from 5.5 h for NaH/DMF literature conditions, down to 2 h. It is worth mentioning that for less reactive substrates, addition of 0.1eq propan-2-ol (i-PrOH) during the first step significantly accelerates the ionization process.

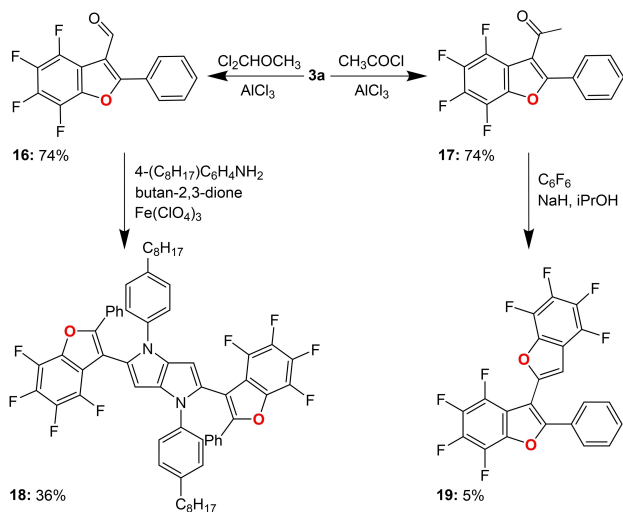
Encouraged by finding optimal conditions, further investigations were focused on expanding the scope of substrates and uncovering possible limitations (Figure 2). Initially, various acetophenones were examined. As it turns out, this reaction is compatible with both electron-donating and electron-withdrawing substituents in the 4-position leading to **3a–e**, with satisfying yields (40%–60%). Moreover, the 2- and  $\alpha$ -substituted acetophenones are also converted with similar efficacy (**5a–c**, **6b,c**), suggesting that the moderate steric hindrance within the carbonyl group does not significantly affect this reaction. However, due to poor solubility of the enolate formed from deoxybenzoin in diglyme, conversion to **6c** was inefficient. Nevertheless, replacement of diglyme by NMP markedly improved enolate solubility, thus increasing reaction yields from 1% up to 67%. It is worth noting that enolizable aldehydes, such as 2-phenyletanal, also undergo this transformation, offering a unique opportunity for 3-substituted  $F_4BF$ s synthesis (**6a**). However, the most outstanding expansion of scope are products originating from acetyl derivatives of pyrrole, furan, thiophene (**7a–c**), pyridine (**8a**) or even ferrocene (**8c**), with the best results obtained for the 2-acetylthiophene. The described transformation also works well for  $\pi$ -expanded methyl-aryl ketones such as naphthalenes and pyrene (**8b, d, e**). Cyclic ketones and their benzo analogs (**9–12**) are also suitable for this method. For example, cyclohexanone is converted to **9** in 48% yield. It turns out that not only perfluorobenzene but also 1,2,4,5-tetrafluorobenzene undergoes this reaction, leading to



**Figure 2.** Scope of the reaction [a] 50 mmol scale, [b] NMP was used, [c] double dilution.

the corresponding difluoroderivative **10b**, although the yield is significantly lower. Undoubtedly, examples deserving special attention are transformations of more than one acetyl group into  $F_4BF$  moieties (**13–15**). During this process, relatively small ketones are converted into  $\pi$ -expanded oligoaryl systems, unattainable by other methodologies. However, due to the multicentric nature of this reaction, their yields range from 8%–18%.

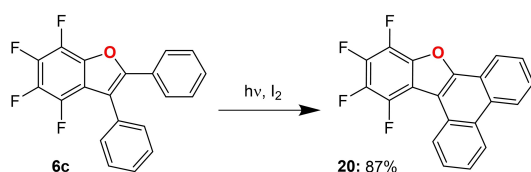
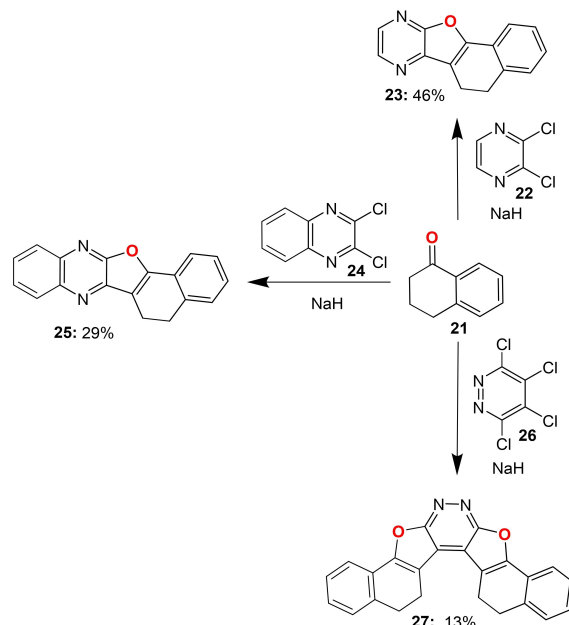
Since the reactivity of fluoroarenes involving fluorine atom nucleophilic substitution ( $S_NAr$ )<sup>[41–43]</sup> or catalytic coupling reactions are well known,<sup>[44]</sup> we decided to investigate their reactivity toward electrophilic substitution ( $S_EAr$ ). It turns out that despite the depletion of the electron density within the  $F_4BF$  core, resulting from the presence of four fluorine atoms, substitution takes place in position 3. Hereby, it is possible to obtain both the aldehyde **16** (74%) and ketone **17** (74%) in good yields (Scheme 2). Compound **16**, when subjected to a multicomponent reaction<sup>[45]</sup> with an amine in the presence of butan-2,3-dione and  $Fe(ClO_4)_3$  is converted into the significantly

Scheme 2. Reactivity of 4,5,6,7-tetrafluorobenzo[*b*]furans.

$\pi$ -expanded system **18** possessing a 1,4-dihydropyrrolo[3,2-*b*]pyrrole core.

Alternatively, the acetyl group present in **17** can be transformed into another  $F_4BF$  moiety (**19**), radically expanding the aromatic system. However, in this case side reactions diminish the yield to around 5%. In addition to electrophilic substitution, appropriately functionalized  $F_4BF$ s undergo other reactions characteristic for arenes. For example, UV irradiation of **6c** in the presence of iodine initiates a  $6\pi$ -electrocyclization, leading to a significantly conjugated  $\pi$ -electron system **20** with an excellent yield of 87% (Scheme 3).

It should be noted that the developed methodology is not limited to the synthesis of fluorinated benzo[*b*]furans. Replacement of perfluorobenzene with other systems capable of  $S_NAr$ , such as 2,3-dichloropyridazines (**22**, **24**), enables conversion of ketones to furo[2,3-*b*]pyridazines (Scheme 4), heteroaromatic systems known for their biological activity.<sup>[46–48]</sup> To the best of our knowledge, methods describing direct conversion of carbonyl compounds to the corresponding furo[2,3-*b*]pyridazines, utilizing  $NaNH_2$ <sup>[49]</sup> or  $KCN$ <sup>[50]</sup> as the ionization agent, lead to furan-fused system with yields of just 2%–8%. In contrast, our synthetic protocol allows us to obtain **23** and **25** in 46% and 29% reaction yield, respectively. Moreover, upon four-fold  $S_NAr$  within pyridazine core **26**, the  $\pi$ -expanded heterohelicene **27** can be easily obtained, the structure of which has been confirmed by X-ray analysis (Figure S6.1, Supporting Information).

Scheme 3. Photocyclization of **6c**.Scheme 4. Synthesis of furo[2,3-*b*]pyridazines.

## Photophysical Properties and Computational Studies

To investigate the influence of fluorine atoms on electronic structure (Figure 3) and spectroscopic properties,  $F_4BF$ s were compared to the reference system 2-phenylbenzofuran (**28**). The majority of the 2-aryl substituted  $F_4BF$ s were characterized by UV-Vis region absorption and emission (Table 2, Figure 4). Furthermore, the presence of four fluorine atoms hypsochromically shifts both spectra compared to **28**, and for 3-aryl derivatives (**6a**, **11**) the observed blue-shift is even more significant. As indicated by DFT calculations, the enlarged energy gap in benzofuran **3a** is a consequence of increased stabilization of the Highest Occupied Molecular Orbital (HOMO) level rather than the Lowest Unoccupied Molecular Orbital (LUMO) (Figure 3 and in Supporting Information Figure S5.3a–g), however the effect is mild due to the largely delocalized character of the frontier orbitals.

The dihedral angles between the 2-aryl substituent and heterocyclic core are often zero in the ground state (Table 3), and when a distortion is found in the ground state the excited state typically results flatter. Upon bridging of the heterocyclic core as in molecule **10a** a small bathochromic shift is observed: this is likely to be the result of multiple effects, since the molecule is less planar respect to **3a** (Table S5.5a–b in Supporting Information). A comparison of the scans for **3a**, **10a** and **28** in Figure S5.4 (Supporting Information) also offers some insight on the sensitivity of the potential energy surface (PES) with respect to this torsion, with the ground state more flat than the first excited state for the non-bridged molecules.

The presence of four fluorine atoms alters the electron-donating character of benzofuran. In these biaryl compounds the presence of an electron-withdrawing group in position 4 of the phenyl substituent induces a negligible bathochromic shift

**Table 2.** Photophysical properties of fluorinated benzofurans in solution.

compound	toluene				dichloromethane			
	$\lambda_{\text{abs}}$ [nm] ( $\epsilon \cdot 10^{-3} \text{ cm}^{-1} \text{ M}^{-1}$ )	$\lambda_{\text{em}}$ [nm]	$\Phi_{\text{fl}}$ [%]	$\Delta\nu$ [ $\text{cm}^{-1}$ ]	$\lambda_{\text{abs}}$ [nm] ( $\epsilon \cdot 10^{-3} \text{ cm}^{-1} \text{ M}^{-1}$ )	$\lambda_{\text{em}}$ [nm]	$\Phi_{\text{fl}}$ [%]	$\Delta\nu$ [ $\text{cm}^{-1}$ ]
<b>3a</b>	299 (25.7), 312 (15.1)	326, 339, 354	54	1400	297 (30.3), 309 (17.4)	321, 337, 354	6.4	1200
<b>3b</b>	301 (35.8), 322 (20.0)	336, 354, 369	54	1300	305 (34.9), 322 (19.4)	337, 354, 369	5.6	1400
<b>3c</b>	344 (40.4)	400	72	4000	344 (40.6)	413	4.7	4850
<b>3d</b>	316 (34.0), 330 (24.0)	349, 365	82	1650	313 (37.4), 328 (25.8)	348, 363	66	1750
<b>3e</b>	321 (41.9)	353, 370, 387	67	2800	318 (43.9)	355, 370, 387	66	3300
<b>5a</b>	298 (24.2), 312 (15.9)	340, 353	10	2600	296 (26.1), 310 (16.1)	333, 347, 364	2.3	2200
<b>5b</b>	298 (21.6), 312 (13.3)	325, 340, 357	5	1300	296 (26.0), 309 (14.7)	325, 337, 354	0.4	1600
<b>5c</b>	299 (25.7), 313 (17.8)	375	8.3	5300	298 (18.5), 312 (11.9)	375	4.0	5400
<b>6a</b>	— <sup>[a]</sup>	— <sup>[a]</sup>	— <sup>[a]</sup>	— <sup>[a]</sup>	241 (10.9)	330	1.0	11200
<b>6b</b>	288 (22.5)	325, 339, 355	18	3950	287 (30.5)	322, 338, 355	3.6	3900
<b>6c</b>	299 (25.0)	357, 375, 396	4.4	5400	298 (22.8)	356, 375, 396	1.5	5500
<b>7a</b>	315 (32.0)	369	19	4650	313 (30.6)	369	2.3	4850
<b>7b</b>	304 (27.8), 319 (19.8)	330, 345, 361	46	1050	302 (30.3), 317 (20.3)	330, 345, 361	1.0	1200
<b>7c</b>	313 (23.1)	373, 384	29	5100	311 (26.0)	373, 384	18	5300
<b>8a</b>	303 (26.8), 317 (23.6)	332, 346, 360	9.4	1400	301 (27.6), 314 (21.9)	329, 342	12	1450
<b>8b</b>	316 (35.2), 330 (27.9)	351, 370, 389	46	1800	313 (36.3), 328 (29.4)	351, 370, 389	40	2000
<b>8c</b>	302 (14.7), 353 (1.4), 454 (0.6)	542	0,001 >	3600	302 (15.4), 353 (1.3), 454 (0.5)	542	0,001 >	3600
<b>8d</b>	315 (18.3)	377, 388	96	5000	315 (17.9)	377, 388	62	5000
<b>8e</b>	368 (34.8)	410, 435	74	2800	366 (34.4)	410, 435	74	2900
<b>9</b>	— <sup>[a]</sup>	— <sup>[a]</sup>	— <sup>[a]</sup>	— <sup>[a]</sup>	253 (9.1)	— <sup>[b]</sup>	— <sup>[b]</sup>	— <sup>[b]</sup>
<b>10a</b>	300 (20.4), 312 (25.7), 327 (20.3)	340, 356, 373	39	1200	299 (24.4), 311 (28.5), 326 (22.3)	338, 355, 372	2.3	1100
<b>10b</b>	319 (29.6), 334 (28.3)	343, 360, 377	71	800	318 (34.7), 333 (33.0)	342, 359, 377	59	800
<b>11</b>	— <sup>[a]</sup>	— <sup>[a]</sup>	— <sup>[a]</sup>	— <sup>[a]</sup>	260 (13.4), 283 (9.1)	339, 356, 373	1.1	5500
<b>12</b>	300 (25.2), 309 (19.4)	329, 343, 360	22	2000	297 (28.0), 309 (20.4)	328, 343, 360	1.8	1900
<b>13</b>	331 (46.7), 346 (62.0), 365 (44.8)	374, 396, 421	92	700	328 (47.6), 342 (63.0), 361 (44.2)	370, 392, 416	82	700
<b>14</b>	— <sup>[a]</sup>	— <sup>[a]</sup>	— <sup>[a]</sup>	— <sup>[a]</sup>	275 (66.2), 316 (17.8)	360, 463	1.9	3900
<b>15</b>	— <sup>[a]</sup>	— <sup>[a]</sup>	— <sup>[a]</sup>	— <sup>[a]</sup>	287 (51.2)	397, 417	1.7	9650
<b>16</b>	312 (10.6)	— <sup>[b]</sup>	— <sup>[b]</sup>	— <sup>[b]</sup>	305 (8.5)	— <sup>[b]</sup>	— <sup>[b]</sup>	— <sup>[b]</sup>
<b>17</b>	— <sup>[a]</sup>	— <sup>[a]</sup>	— <sup>[a]</sup>	— <sup>[a]</sup>	293 (16.3)	— <sup>[b]</sup>	— <sup>[b]</sup>	— <sup>[b]</sup>
<b>18</b>	372 (12.4)	478	37	6000	371 (9.0)	510	31	7350
<b>19</b>	— <sup>[a]</sup>	— <sup>[a]</sup>	— <sup>[a]</sup>	— <sup>[a]</sup>	305 (16.5)	421	23	9000
<b>20</b>	308 (15.1), 320 (15.0), 338 (1.9), 355 (1.7)	356, 375, 395	24	100	306 (19.4), 318 (17.7), 337 (2.9), 353 (2.4)	356, 375, 395	14	200
<b>23</b>	347 (28.0), 359 (25.3)	385, 397	77	1900	348 (27.0), 358 (25.0)	410	90	3500
<b>25</b>	379 (31.4), 398 (28.2)	418, 439	78	1200	380 (30.5), 398 (26.8)	430, 448	50	1900
<b>27</b>	377 (22.1), 392 (42.6), 416 (52.1)	422, 450, 474	100	300	379 (24.6), 394 (46.6), 418 (55.3)	424, 452, 477	81	300
<b>28</b>	306 (21.7), 320 (19.2)	327, 343, 360	13	700	304 (30.2), 318 (21.0)	327, 343, 360	77	900

$\lambda_{\text{abs}}$ ,  $\lambda_{\text{em}}$  – absorption and emission wavelength,  $\epsilon$  – molar absorption coefficients,  $\Phi_{\text{fl}}$  – quantum yield,  $\Delta\nu$  – Stokes shift, [a] due to toluene absorption, determination of compound spectroscopic data was impossible, [b] fluorescence below detection limit.

of absorption, whereas the Me<sub>2</sub>N group shifts emission by approx. 50 nm in toluene (**3a** vs. **3c** vs. **3d**, Table 1) effectively leading to blue fluorescence for dye **3c**. Calculations reveal more details about the push-pull nature of chromophore **3c**. It possesses typical features of a donor-acceptor system, where the fluorinated moiety acts as an acceptor. A charge separation upon excitation is observed, however due to the delocalization

of the S<sub>1</sub> state (as mainly described by HOMO-LUMO, Figure 3, Table S5.7 in Supporting Information) the effect is weak. This interpretation is consistent with computed large state electric dipole moment ( $\mu(S_0)$ ) which is further increased upon excitation to S<sub>1</sub>, as well as the strong collinearity of both  $\mu(S_0)$  and  $\mu(S_1)$  along the vector connecting acceptor and donor subunit (Table S5.4b). Moreover, upon rising the solvent polar-

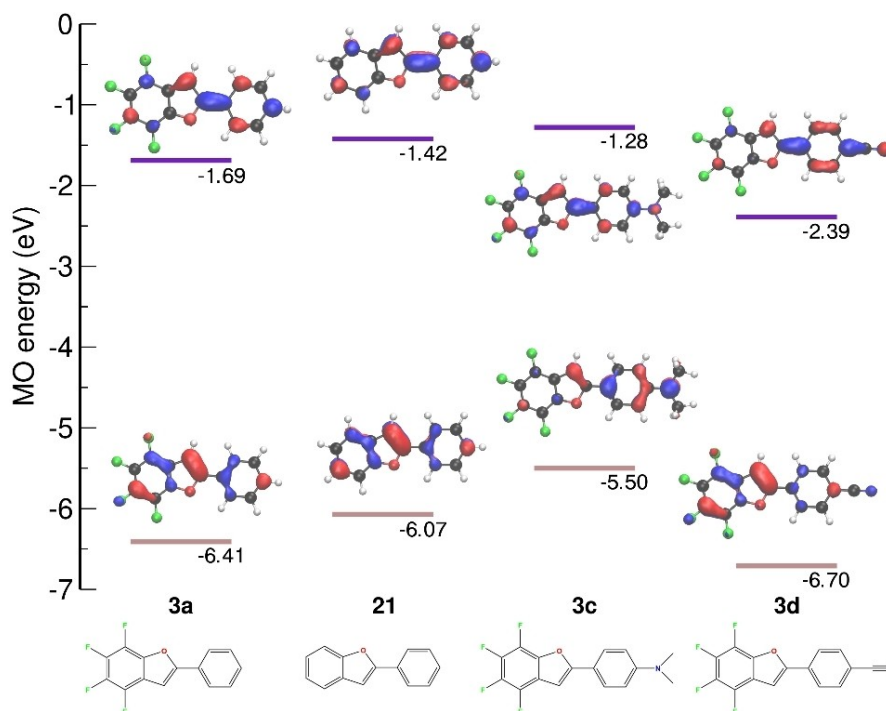


**Figure 3.** Calculated energy diagram of **3a**, **3c**, **3d** and **28** calculated with DFT PBE0/def2-TZVP D3(BJ) in toluene (CPCM) and orbitals figures with isosurface value  $\pm 0.05$ .

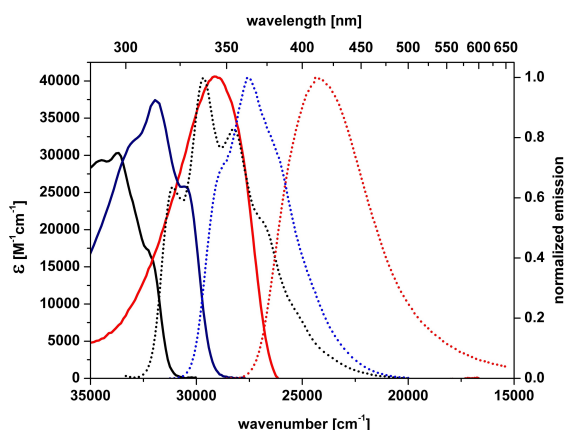


**Figure 4.** Absorption (solid) and emission (dot) spectra of **3a** (black), **3c** (red) and **3d** (blue) in dichloromethane.

ity,  $S_1 \rightarrow S_0$  transition energies decrease while  $\mu(S_1)$  becomes larger (Table S5.4a). It is worth noting that switching from toluene to dichloromethane, **3c** fluorescence quantum yield ( $\Phi_f$ ) decreases 15-times. Similar behavior is observed for molecules **3a**, **7a**, **7b** and **10a**. In all these systems, as suggested by the magnitude and orientation of the dipole moments, similar for ground and excited states, the delocalized character is conserved (Tables S5.4a and b). This would suggest some sensitivity to the rotation around the biaryl torsional angle as a possible mechanism for which a larger  $\Phi_f$  is observed in a more viscous solvent. This effect is not observed in **3d**, which is highly emissive in both toluene and dichloro-

**Table 3.** Computed oscillator strengths for  $S_0 \rightarrow S_1$  transition and dihedral angles in  $S_0$  and  $S_1$  states for exemplary  $F_4BF_5$ s.

compound	dih. angle $S_0$ ( $q_0$ , toluene)	dih. angle $S_1$ ( $q_1$ , toluene)	$f$ (toluene)	$f$ ( $CH_2Cl_2$ )
<b>3a</b>	0.25	0.00	1.247	1.378
<b>3c</b>	2.02	0.21	1.580	1.657
<b>3d</b>	1.17	0.35	1.330	1.477
<b>6a</b>	41.77	5.90	1.145	1.298
<b>7a</b>	5.96	1.46	1.299	1.379
<b>7b</b>	4.26	0.73	1.331	1.400
<b>8a</b>	4.26	1.92	1.147	1.477
<b>10a</b>	12.42	4.70	0.267	0.357
<b>25</b>	3.04	4.11	1.058	1.199
<b>27</b>	2.61	3.81	1.659	1.754
<b>28</b>	0.94	0.30	1.265	1.389

$f$  – oscillator strength for  $S_0 \rightarrow S_1$  transition.

methane. Molecule **3d** features dipolar character due to the strong withdrawing power of the CN group, which is also clear in the orbital energies (Figure 3). Calculations indicate that **3d**  $\mu(S_0)$  vector orientation is opposite to the one observed in **3c**, proving that in **3d** fluorinated benzofuran acts as donating subunit. Besides, as opposed to **3c**, in **3d**  $\mu(S_1)$  is rotated by approx.  $30^\circ$  with respect to  $\mu(S_0)$ . A similar charge rearrangement upon excitation is also observed for **8a**, in which the electric dipole moment is rotated by approx.  $50^\circ$  (again in Table S5.4b). Both of these systems exhibit a similar  $\Phi_f$  for the two investigated solvents.

On the other hand, for the more complex oligoaryl systems **14** and **15**, an hypsochromic shift is observed. Due to

insufficient conjugation between the highly twisted  $\pi$ -electron subunits, the range of absorbed light falls within the UV region. A characteristic feature of  $F_4BF$ s is a large Stokes shift, which is at least twice as large as that for the reference system **28**; about  $1300\text{ cm}^{-1}$  for simple systems, and for example  $5000\text{ cm}^{-1}$  for compound **8d** possessing a naphthalen-1-yl substituent.

The rotation along the biaryl linkage is expected to strongly modulate the extent of the conjugation. In particular, LUMO orbitals involved in the excitation possess strong bonding character across the inter-ring bond. Besides, the substitution pattern heavily affects the electronic structure, and both transition energies and dipole moments change. For simple 2-substituted  $F_4BF$ s, the molar absorption coefficient is in the range of  $20000\text{--}40000\text{ cm}^{-1}\text{ M}^{-1}$ , while for 3-substituted  $F_4BF$ s, it ranges from  $10000$  to  $15000\text{ cm}^{-1}\text{ M}^{-1}$ , with strongly blue-shifted absorption (wavelength  $< 250\text{ nm}$ ). Calculated oscillator strengths are in line with these experimental results, which for 2-substituted derivatives are about 1.2 while for 3-substituted  $F_4BF$ s, they are around 5 times smaller (Table 3, Tables S5.1–S5.3). For most 2-substituted systems, high oscillator strengths translate into good emissive properties. The observed  $\Phi_{fl}$  in toluene range from about 30% up to over 90% in the case of **8d** and **13**. Moreover, changing the solvent to a more polar one, for example dichloromethane, is often accompanied by a 20-fold decrease in  $\Phi_{fl}$ , which is the opposite effect compared to the nonfluorinated system **28**. This phenomenon does not occur in more complex  $\pi$ -electron systems. Excited-state relaxation of vibrational and solvent degrees of freedom translates into different effectiveness of non-radiative decay paths.

Among all studied species, molecule **6a** exhibits markedly unique behavior, including a large Stokes shift ( $11200\text{ cm}^{-1}$ ) and very low  $\Phi_{fl}$ . This is a result of a different substitution position which hinders conjugation between the aryl moiety and fluorinated subunit, causing high distortion and thus destabilizing the LUMO (Tables S5.6 and S5.7), which translates into a blueshift in the absorption spectrum. It is worth mentioning that the first electron transition also features a smaller HOMO-LUMO contribution relative to the 2-substituted  $F_4BF$ s.

Except for the case of **6a**, where calculations report large torsion angle change from approx.  $41^\circ$  in the ground state to  $\sim 5^\circ$  for the first excited state (Table 3), the calculated structural difference between ground state and relaxed excited state are quite modest in all the systems. Therefore, we expect that the observation of large Stokes shifts is a consequence of detailed solvation effects, possibly connected with the significant acquired polarized character upon excitation (see excited state dipole moment in Table S5.4a. and Table 3).

For 2-substituted  $F_4BF$ s, Time-Dependent DFT (TDDFT) calculations with the PBE0 functional<sup>[51]</sup> render the first excited state markedly bright, with a transition dipole moment oriented parallel to the inter-ring molecular axis. This excitation shows a dominant HOMO→LUMO character with a weight of around 97% for all systems (Table S5.7).

$\pi$ -Expansion of the aryl substituent at position 2 (e.g., pyrenyl, **3a**→**8e**) leads to a bathochromic shift of absorption ( $\approx 50\text{ nm}$ ) and of emission ( $\approx 80\text{ nm}$ ). Linking two  $F_4BF$  units via

a 1,4-phenylene subunit leads to a marked bathochromic shift of absorption and emission (**13** vs. **3a**) and provides an increase of  $\Phi_{fl}$  to near quantity (Table 1).

Comparing the  $F_4BF$  spectroscopic data, it can be noticed that dye **20** meaningfully differs from other systems. Apart from the small Stokes shift ( $100\text{ cm}^{-1}$ ), a characteristic feature is the presence of low-energy absorption bands with low intensity. To understand this behavior, we can consider a molecule of **20** as a system derived from  $D_{3h}$  symmetric triphenylene, in which one benzene ring has been replaced by a benzo[*b*]furan subunit. The first two triphenylene electronic transitions are symmetry-forbidden,<sup>[52]</sup> however, despite the symmetry breaking, the  $S_0\rightarrow S_1$  and  $S_0\rightarrow S_2$  transitions in **20** still clearly possess forbidden character. This phenomenon is also observed for other compounds derived from highly symmetric systems<sup>[53]</sup> and leads to a characteristic increase in the fluorescence quantum yield, in this case from 9% for triphenylene to 24% for **20**.

Solid-state spectroscopy provides additional information on the photophysical properties of  $F_4BF$ s (Table 4). Comparison of  $F_4BF$  spectra in toluene versus the crystalline state indicates a clear red-shift from  $1200\text{ cm}^{-1}$  for simple derivatives, up to  $5500\text{ cm}^{-1}$  for the more complex systems **8e** and **13**, which suggests strong intermolecular interactions in the condensed phase. It should be mentioned that most of the measured emission quantum yields range from 25% to 55%. Particularly pronounced decreases observed for **8e** and **13**, from 74% and 92% in solution to 23% and 31% in the solid state, respectively, are a consequence of both the reabsorption of the emitted radiation and the non-radiative energy dissipation in a highly aggregated environment. While strong intermolecular interactions lower emissive properties, they may be particularly important in the case of electric charge mobility. Thus, properly functionalized  $F_4BF$ s might prove a valuable and readily available class of organic semiconductors.

Particularly noteworthy are furo[2,3-*b*]pyrazines **23** and **25**, as well as helical pyridazine **27**, for which the largest computed oscillator strengths for both absorption (1.7) and emission (1.9) are observed. These compounds are characterized by large blue fluorescence quantum yields exceeding 80%, narrow full width at half maximum (FWHM) (**23**: 0.45 eV, **25**: 0.43 eV), and good color purity (CIE 1931; **23**: [0.16, 0.03], **25**: [0.15, 0.08]). Such

**Table 4.** Photophysical characterization of  $F_4BF$  in crystalline state.

compound	$\lambda_{ex}$ [nm]	$\lambda_{em}$ [nm]	$\Phi_{fl}$ [%]	$\Delta\nu$ [ $\text{cm}^{-1}$ ]
<b>3a</b>	324	360	43	3100
<b>7a</b>	343	410	25	4800
<b>7b</b>	343	405	4.4	4500
<b>7c</b>	349	411, 436	30	4300
<b>8a</b>	330	366, 379	8.5	3000
<b>8e</b>	472	517	23	1850
<b>10a</b>	340	376, 387	55	2800
<b>10b</b>	354	385	42	2300
<b>11</b>	324, 339	362	7.8	1900
<b>13</b>	424	468	31	2200
<b>28</b>	354	380	76	1900

$\lambda_{ex}$ ,  $\lambda_{em}$  – excitation and emission wavelength,  $\Phi$  – quantum yield,  $\Delta\nu$  – Stokes shift.



spectral characteristics fulfill the requirements for blue OLED emitters, making furo[2,3-*b*]pyrazines a competitive and desirable class of emissive materials.<sup>[54]</sup> As shown in Figure S5.3(a and b) (Supporting Information), both HOMO and LUMO in dye **25** conserve delocalized character with similar isosurface patterns for furan moiety compared to compound **28**. In the molecule of **27** we observe a symmetric combination for the HOMO and anti-symmetric for the LUMO with respect to **28**. In both **25** and **27** a large stabilization of LUMO levels is observed in comparison with **28**, which suggests potential use of those substances as Electron Transporting Materials (ETM).

## Conclusion

A safe and straightforward protocol for transformation of compounds possessing -CH<sub>2</sub>CO- functionality into 4,5,6,7-tetrafluorobenzofurans was developed. It has been proven that aryl-alkyl ketones can act as double O,C-nucleophiles. The presented synthetic methodology enables the direct, efficient, and large-scale conversion of enolizable ketones and aldehydes into the corresponding 2- and 3-substituted F<sub>4</sub>BFs, as well as  $\alpha$ -pentafluorophenyl ketones. The described transformation is suitable for acetophenone derivatives decorated with both donor and acceptor substituents, as well as 5- and 6-membered heterocyclic systems, ferrocene derivatives and extended aromatic hydrocarbons. Moreover, utilizing other systems prone to double-S<sub>N</sub>Ar reaction, such as 1,2,4,5-tetrafluorobenzene, 2,3-dichloropyrazines and 3,4,5,6-tetrachloropyridazine, undoubtedly expands applicability of this transformation. The vast scope of substrates makes this reaction an alternative to the Suzuki reaction, allowing the introduction of F<sub>4</sub>BF subunits to many unique architectures. On the other hand, simple post-functionalization of the obtained systems leads to previously inaccessible fluoroarenes. Good emissive properties, as well as high aggregation in the solid state, make F<sub>4</sub>BFs an interesting class of substances with potential applications in optoelectronics as emitters and organic semiconductors. We have rationalized their properties based on a detailed computational study on the isolated molecules (in implicit solvent). Moreover, properly functionalized F<sub>4</sub>BFs should also be considered in terms of pharmacological activity. As the fluorine atom is a bioisostere of the hydrogen atom, comparison of the durability and pharmacological activity of traditional versus fluorinated benzo[*b*]furan-based drugs are worthy of further attention and can now be carried out in a simple and effective manner. The broad scope of this method enables the construction of a plethora of 4,5,6,7-tetrafluorobenzofurans possessing one or two substituents at positions 2 and 3.

## Experimental Section

For general information, all experimental, analytical, spectral, X-ray structure and computational details see Supporting Information.

**Computation:** Electronic structure calculations of functionalized F<sub>4</sub>BFs were performed using Density Functional Theory (DFT) and

Time-Dependent DFT (TDDFT) calculations on a selected set of molecules in this work, namely **3 a**, **3 c**, **3 d**, **6 a**, **7 a**, **7 b**, **8 a**, **10 a**, **25**, **27**, **28**. We employed the PBE0 functional with a def2-TZVP basis set and Grimme's D3(BJ) correction in the ORCA 5.0 package.<sup>[51,55–58]</sup> Ground and first excited-state geometries were optimized using a continuum-solvent model.<sup>[59,60]</sup> Transition properties (energies and transition dipole moments) were calculated to simulate absorption and emission, along with ground and excited state (permanent) dipole moments at the relaxed geometries. The latter moments were analyzed in terms of magnitude and directions. For this purpose, we defined a reference vector and we computed the angle formed from electric state dipole moment with respect to this one, as sketched in the Figure S5.1-2 (Supporting Information). In the Supporting Information, we also report dipole moment magnitude for ground and excited state at their equilibrium geometries (Table S5.4), and the angle formed with the above reference vector (Table S5.4b).

**General procedure of 4,5,6,7-tetrafluorobenzo[*b*]furans synthesis:** To 100 mL Schlenk flask under Ar atmosphere, sodium hydride<sup>[a]</sup> (25 mmol, 60% in mineral oil) and ketone (10 mmol) were added, then 5 mL<sup>[b]</sup> of dry THF and 2-propanol<sup>[a]</sup> (1 mmol) was introduced and reaction temperature was raised to 60 °C – the solution slowly turned yellow/orange/brown and a colorless gas was evolved. After 1 h perfluorobenzene<sup>[a]</sup> (15 mmol) was added and the mixture was stirred by additional 1 h in constant temperature, whereupon 10 mL<sup>[b]</sup> of diglyme was added and after the evolution of colorless gas from the dark brown mixture had ceased, the excess volatiles was evaporated under 60 °C and reduced pressure. After complete evaporation of THF and perfluorobenzene the ambient gas atmosphere was restored and then the temperature of the reaction mixture was raised to 170 °C – the mixture darkened. After 1 h, it was cooled to room temperature, 40 mL of water was added, and the formed solid was filtered off and washed with water. Then it was dissolved in DCM, dried over MgSO<sub>4</sub> and evaporated. The crude product was adsorbed at 10 g of silica gel and then purified via column chromatography (SiO<sub>2</sub>, 50 g). [a] in the case of dicarbonyl compounds: 5 equiv. of NaH, 2 equiv. of perfluorobenzene and 0.2 equiv. 2-propanol were used; [b] in case of **8 a**, **14** and **15** double dilution was used.

## Acknowledgements

The work was financially supported by the Polish National Science Centre, Poland (HARMONIA 2018/30/M/ST5/00460), the Foundation for Polish Science (TEAM POIR. 04.04.00-00-3CF4/16-00). We acknowledge European Union's Horizon 2020 research and innovation programme under the Marie Skłodowska-Curie grant agreement No 101007804 (Micro4Nano). L.G. and T.O. acknowledge the Croatian Science Foundation (HrZZ), via the project IP-2020-02-7262 (HYMO4EXNOMOMA). The Advanced Light Source (ALS) is supported by the Director, Office of Science, Office of Basic Energy Sciences, of the U.S. DOE under contract no. DE-AC02-05CH11231

## Conflict of Interest

The authors declare no conflict of interest.

## Data Availability Statement

The data that support the findings of this study are available in the supplementary material of this article.

**Keywords:** benzofuran · donor-acceptor systems · dyes/pigments · fluorescence · ketones

- [1] S. Khanam Hena, *Eur. J. Med. Chem.* **2015**, *97*, 483–504.
- [2] Y. Miao, Y. Hu, J. Yang, T. Liu, J. Sun, X. Wang, *RSC Adv.* **2019**, *9*, 27510–27540.
- [3] C. B. Nielsen, T. Brock-Nannestad, T. K. Reenberg, P. Hammershøj, J. B. Christensen, J. W. Stouwdam, M. Pittelkow, *Chem. Eur. J.* **2010**, *16*, 13030–13034.
- [4] C. B. Nielsen, T. Brock-Nannestad, P. Hammershøj, T. K. Reenberg, M. Schau-Magnussen, D. Trpcević, T. Hensel, R. Salcedo, G. V. Baryshnikov, B. F. Minaev, M. Pittelkow, *Chem. Eur. J.* **2013**, *19*, 3898–3904.
- [5] K. Górski, J. Mech-Piskorz, K. Noworyta, B. Leśniewska, M. Pietraszkiewicz, *New J. Chem.* **2018**, *42*, 5844–5852.
- [6] K. Mitsudo, Y. Kobashi, K. Nakata, Y. Kurimoto, E. Sato, H. Mandai, S. Suga, *Org. Lett.* **2021**, *23*, 4322–4326.
- [7] L. Đorđević, D. Milano, N. Demitri, D. Bonifazi, *Org. Lett.* **2020**, *22*, 4283–4288.
- [8] P. M. Byers, J. I. Rashid, R. K. Mohamed, I. V. Alabugin, *Org. Lett.* **2012**, *14*, 6032–6035.
- [9] H. S. Prakash Rao, S. Vijjapu, *RSC Adv.* **2014**, *4*, 25747–25758.
- [10] M. Shi, Y. He, Y. Sun, D. Fang, J. Miao, M. U. Ali, T. Wang, Y. Wang, T. Zhang, H. Meng, *Org. Electron.* **2020**, *84*, 105793.
- [11] Q. Zhang, Y. Wang, S. J. Yoon, W. J. Chung, S. Ye, R. Guo, P. Leng, S. Sun, J. Y. Lee, L. Wang, *J. Mater. Chem. C* **2020**, *8*, 1864–1870.
- [12] D. Chen, J. Li, W. Ma, B. Li, Y. Zhen, X. Zhu, W. Hu, H. Tsuji, E. Nakamura, *Asian J. Org. Chem.* **2018**, *7*, 2228–2232.
- [13] J. Faragó, A. Kotschy, *Synthesis* **2009**, *2009*, 85–90.
- [14] Y. Komine, A. Kamisawa, K. Tanaka, *Org. Lett.* **2009**, *11*, 2361–2364.
- [15] L. Arias, Y. Vara, F. P. Cossio, *J. Org. Chem.* **2012**, *77*, 266–275.
- [16] A. A. Abu-Hashem, H. A. R. Hussein, A. S. Aly, M. A. Gouda, *Synth. Commun.* **2014**, *44*, 2285–2312.
- [17] L. Politanskaya, E. Tretyakov, C. Xi, *J. Fluorine Chem.* **2021**, *242*, 109720.
- [18] L. Politanskaya, N. Troshkova, E. Tretyakov, C. Xi, *J. Fluorine Chem.* **2019**, *227*, 109371.
- [19] L. Politanskaya, V. Shteingarts, E. Tretyakov, A. Potapov, *Tetrahedron Lett.* **2015**, *56*, 5328–5332.
- [20] L. V. Politanskaya, I. P. Chuikov, E. V. Tretyakov, V. D. Shteingarts, L. P. Ovchinnikova, O. D. Zakharova, G. A. Nevinsky, *J. Fluorine Chem.* **2015**, *178*, 142–153.
- [21] L. V. Politanskaya, I. P. Chuikov, V. D. Shteingarts, *Tetrahedron* **2013**, *69*, 8477–8486.
- [22] L. Politanskaya, T. Rybalova, O. Zakharova, G. Nevinsky, E. Tretyakov, *J. Fluorine Chem.* **2018**, *211*, 129–140.
- [23] Q. Deraedt, L. Marcélis, T. Auvray, G. S. Hanan, F. Loiseau, B. Elias, *Eur. J. Inorg. Chem.* **2016**, *2016*, 3649–3658.
- [24] A. Heaton, M. Hill, F. Drakesmith, *J. Fluorine Chem.* **1997**, *81*, 133–138.
- [25] G. M. Brooke, W. K. R. Musgrave, T. R. Thomas, *J. Chem. Soc. C Org.* **1971**, 3596.
- [26] R. Filler, S. M. Woods, W. L. White, *Can. J. Chem.* **1989**, *67*, 1837–1841.
- [27] W.-S. Ojo, K. Jacob, E. Despagnet-Ayoub, B. K. Muñoz, S. Gonell, L. Vendier, V.-H. Nguyen, M. Etienne, *Inorg. Chem.* **2012**, *51*, 2893–2901.
- [28] E. J. Gruver, E. O. Onyango, G. W. Gribble, *Arkivoc* **2018**, *2018*, 144–152.
- [29] L. Zhu, M. Zhang, *J. Org. Chem.* **2004**, *69*, 7371–7374.
- [30] G. L. Silva, V. Ediz, D. Yaron, B. A. Armitage, *J. Am. Chem. Soc.* **2007**, *129*, 5710–5718.
- [31] Z. Xu, H. Chen, G.-J. Deng, H. Huang, *Org. Lett.* **2021**, *23*, 936–942.
- [32] R. Wang, H. Lu, M. Yan, M. Li, X. Lv, H. Huang, A. Ghaderi, T. Iwasaki, N. Kambe, A. Abdukader, R. Qiu, *J. Mater. Chem. C* **2021**, *9*, 12545–12549.
- [33] M. D. Castle, R. G. Plevy, J. C. Tatlow, *J. Chem. Soc. C* **1968**, 1225–1227.
- [34] J.-C. Blazejewski, C. Wakselman, *J. Chem. Soc. Perkin Trans. 1* **1980**, 2845–2850.
- [35] M. Arisawa, S. Nakane, M. Kuwajima, M. Yamaguchi, *Heterocycles* **2012**, *86*, 1103–1118.
- [36] J. Schwaben, N. Münster, M. Klues, T. Breuer, P. Hofmann, K. Harms, G. Witte, U. Koert, *Chem. Eur. J.* **2015**, *21*, 13758–13771.
- [37] L. K. Hiscock, K. E. Maly, L. N. Dawe, *Cryst. Growth Des.* **2019**, *19*, 7298–7307.
- [38] Y. Inukai, T. Sonoda, H. Kobayashi, *Bull. Chem. Soc. Jpn.* **1979**, *52*, 2657–2660.
- [39] J. Buckley, R. Lee Webb, T. Laird, R. J. Ward, *Chem. Eng. News* **1982**, *60*, 5.
- [40] G. DeWall, *Chem. Eng. News* **1982**, *60* (5), 43.
- [41] J. Li, G. Zhang, D. M. Holm, I. E. Jacobs, B. Yin, P. Stroeve, M. Mascal, A. J. Moulé, *Chem. Mater.* **2015**, *27*, 5765–5774.
- [42] H. A. M. Biemans, C. Zhang, P. Smith, H. Kooijman, W. J. J. Smeets, A. L. Spek, E. W. Meijer, *J. Org. Chem.* **1996**, *61*, 9012–9015.
- [43] V. A. Pistritto, M. E. Schutzbach-Horton, D. A. Nicewicz, *J. Am. Chem. Soc.* **2020**, *142*, 17187–17194.
- [44] J. He, K. Yang, J. Zhao, S. Cao, *Org. Lett.* **2019**, *21*, 9714–9718.
- [45] M. Tasiar, O. Vakuliuk, D. Koga, B. Koszarna, K. Górski, M. Grzybowski, Ł. Kielesiński, M. Krzeszewski, D. T. Gryko, *J. Org. Chem.* **2020**, *85*, 13529–13543.
- [46] D. S. Chekmarev, S. V. Shorshnev, A. E. Stepanov, A. N. Kasatkin, *Tetrahedron* **2006**, *62*, 9919–9930.
- [47] A. Nakhii, M. S. Rahman, G. P. K. Seerapu, R. K. Banote, K. L. Kumar, P. Kulkarni, D. Haldar, M. Pal, *Org. Biomol. Chem.* **2013**, *11*, 4930–4934.
- [48] K. Mohan Saini, S. Kumar, M. Patel, R. K. Saunthwal, A. K. Verma, *Eur. J. Org. Chem.* **2017**, *2017*, 3707–3715.
- [49] J. Jaung, M. Matsuoka, K. Fukunishi, *J. Chem. Res.* **1998**, 284–285.
- [50] E. Hayashi, A. Utsunomiya, *Yakugaku Zasshi* **1975**, *95*, 774–777.
- [51] C. Adamo, V. Barone, *J. Chem. Phys.* **1999**, *110*, 6158–6170.
- [52] S. Kyushin, H. Fujii, K. Negishi, H. Matsumoto, *Mendeleev Commun.* **2022**, *32*, 87–90.
- [53] K. Górski, K. Noworyta, J. Mech-Piskorz, *RSC Adv.* **2020**, *10*, 42363–42377.
- [54] S. S. Reddy, V. G. Sree, H.-Y. Park, A. Maheshwaran, M. Song, S.-H. Jin, *Dyes Pigm.* **2017**, *145*, 63–71.
- [55] F. Neese, *WIREs Comput. Mol. Sci.* **2012**, *2*, 73–78.
- [56] F. Weigend, R. Ahlrichs, *Phys. Chem. Chem. Phys.* **2005**, *7*, 3297–3305.
- [57] S. Grimme, S. Ehrlich, L. Goerigk, *J. Comput. Chem.* **2011**, *32*, 1456–1465.
- [58] S. Grimme, J. Antony, S. Ehrlich, H. Krieg, *J. Chem. Phys.* **2010**, *132*, 154104.
- [59] S. Hirata, M. Head-Gordon, *Chem. Phys. Lett.* **1999**, *314*, 291–299.
- [60] V. Barone, M. Cossi, *J. Phys. Chem. A* **1998**, *102*, 1995–2001.

Manuscript received: November 8, 2022

Accepted manuscript online: January 25, 2023

Version of record online: March 8, 2023